Editors' Suggestion

# Effect of modest hydrostatic pressure on low-temperature transport behavior in $La_3Ni_2O_7$ thin films

Deepak Kumar,[1] Jared Z. Dans,[1] Keenan E. Avers,[1] Ryan Paxson,[1,2]
Ichiro Takeuchi,[1,2] and Johnpierre Paglione[1,3,*]
[1]Maryland Quantum Materials Center and Department of Physics, University of Maryland, College Park, Maryland 20742, USA
[2]Department of Materials Science and Engineering, University of Maryland, College Park, Maryland, USA
[3]Canadian Institute for Advanced Research, Toronto, Ontario M5G 1Z8, Canada

(Received 18 March 2026; accepted 7 July 2026; published 24 July 2026)

The discovery of superconductivity in bilayer nickel oxides has revived an intense effort to understand the potential of high-temperature superconductivity in these materials and their relation to cuprate superconductors. In this work, we investigate the growth and properties of bilayer $La_3Ni_2O_7$ thin films as a function of substrate, oxygen treatment, and applied pressure in order to study the evolution of transport properties. We report epitaxial growth of $La_3Ni_2O_7$ thin films on $LaAlO_3$ (LAO) (001) and $SrLaAlO_4$ (SLAO) (001) substrates, and the effects of *ex situ* annealing in a high-pressure furnace under an oxygen-rich environment (15 bar). Transport measurements show that the $La_3Ni_2O_7$ thin films on LAO(001) exhibit Fermi-liquid-like metallic behavior with a slight Kondo-like upturn at low temperatures, which evolves with the application of modest hydrostatic pressures toward non-Fermi-liquid behavior with a temperature dependence of resistance approaching $\sim T^{1.4}$ at 1.41 GPa. The ability to tune the normal state resistivity of $La_3Ni_2O_7$ films to display non-Fermi-liquid behavior under such a modest hydrostatic pressure range—only 6–8 % of that typically applied via diamond anvil cell in $La_3Ni_2O_7$ single crystals to achieve comparable effects—is both noteworthy and unexpected. These findings imply the strong tunability of $La_3Ni_2O_7$ thin film under epitaxial strain and hydrostatic pressure leading to exotic transport behavior at low temperatures.

DOI: 10.1103/zjnc-vv8p

## I. INTRODUCTION

The discovery of superconductivity in the infinite-layer nickelates in 2019 [1] has sparked significant interest across the scientific community, leading to a surge of dedicated research efforts. The emergence of superconductivity in nickelates materials ($Ni^{1+}$, $3d^9$ electronic configuration), with electronic structures akin to the extensively studied cuprates ($Cu^{2+}$, $3d^9$ electronic configuration), had been anticipated for several decades but had not been observed until recently. This advancement represents a pivotal milestone for the field and introduces both new opportunities and challenges for elucidating the mechanisms underlying high-transition-temperature ($T_c$) superconductivity. Among these compounds, the Ruddlesden-Popper (RP) bilayer nickelate $La_3Ni_2O_7$ stands out as the most recently identified high-$T_c$ superconductor, exhibiting an onset $T_c$ near 80 K in bulk crystals subjected to 14 GPa of external pressure [2]. The presence of structural polymorphs, including various RP variants, presents substantial obstacles to achieving superconductivity in nickelates, often impeding the realization of a zero-resistance state [3]. Subsequent studies have demonstrated that partial substitution of La with Pr, or the introduction of small amounts of Sr, mitigates the formation of intergrowth phases, enhances the bilayer RP structure conducive to superconductivity, and increases the superconducting volume fraction [4]. Nevertheless, the necessity of applying high pressure to induce superconductivity in $La_3Ni_2O_7$ crystals remained a considerable limitation for experimental investigations into the underlying mechanisms.

Recent advancements have addressed this challenge, with the observation of ambient-pressure superconductivity in $La_3Ni_2O_7$, $(La,Pr)_3Ni_2O_7$, $La_{3-x}Sr_xNi_2O_7$, and $(La,Pr,Sm)_3Ni_2O_7$ thin films grown under compressive strain on $SrLaAlO_4$ (001) substrates, seemingly eliminating the need for high-pressure conditions in these systems [5–8]. Superconductivity in these films has so far only been observed in those annealed with ozone or grown in an ozone-rich environment, while the pristine, untreated films tend to be either insulating or metallic. Additionally, even pristine films that do not exhibit superconductivity under normal conditions can display such superconducting properties when subjected to high pressure [9]. This makes it essential to investigate the specific roles of $O_2/O_3$ and external pressure in bilayer RP thin films. In this work, we present our study on $La_3Ni_2O_7$ thin films prepared under various strain conditions, emphasizing the role of ozone in achieving superconductivity in nickelate films and demonstrating how applied pressure influences their low-temperature properties. Specifically, we show that there is a change in the power-law behavior of the transport measurement, resulting in non-Fermi-liquid behavior for the $La_3Ni_2O_7$ thin film under modest hydrostatic pressure.

## II. EXPERIMENT

$La_3Ni_2O_7$ thin films were fabricated on $LaAlO_3$ (001), $SrLaAlO_4$ (001), and $YAlO_3$ (110) substrates by using pulsed

*Contact author: paglione@umd.edu

 

laser deposition. Ablation of polycrystalline $La_3Ni_2O_7$ and $SrTiO_3$ targets was performed using a KrF excimer laser (248 nm). The $SrTiO_3$ here served as the capping layer to $La_3Ni_2O_7$ film. The laser frequency was set to 5 Hz for $La_3Ni_2O_7$ and 2 Hz for $SrTiO_3$, with corresponding fluences of 0.5 J/cm$^2$ and 0.6 J/cm$^2$. Prior to deposition, $LaAlO_3$ and $YAlO_3$ substrates were annealed at 800°C under $10^{-5}$ torr of $O_2$ for 30 min, while $SrLaAlO_4$ substrates were treated following recipe in Ref. [10], to achieve atomically flat surfaces. Substrate temperatures were maintained at 750°C for the $La_3Ni_2O_7$ layer and 650°C for the $SrTiO_3$ layer. Oxygen partial pressures during growth were adjusted to 100 mtorr for $La_3Ni_2O_7$ and 150 mtorr for $SrTiO_3$, with a fixed target-to-substrate distance of 5 cm. Postdeposition, the films were annealed briefly at 650°C, 80 torr for 10 min. Film characterization was conducted using x-ray diffraction with a Rigaku diffractometer equipped with a monochromated Cu $K\alpha1$ radiation source ($\lambda = 1.5406$ Å). Temperature-dependent resistance measured via the four-probe method, and Hall effect measurements under ambient pressure were performed using a physical property measurement system (PPMS, Quantum Design). For high-pressure oxygen treatment, samples were put into ceramic crucibles, placed within a quartz tube in a GSL-1100X-RC high-temperature, high-pressure furnace, and annealed for 18 h at an oxygen pressure of 15 bar. High-pressure measurements (up to 1.41 GPa) were carried out on $La_3Ni_2O_7$ thin films on LAO substrate (1.5 × 3 mm$^2$) using a piston-cylinder cell (PCC) with Daphne 7575 oil as the pressure-transmitting medium. The pressure was determined *in situ* with a Pb manometer.

## III. RESULTS AND DISCUSSION

Figure 1 presents an overview of the structural characterization of 6–7 nm $La_3Ni_2O_7$ ($LNO_{327}$) thin films deposited on $LaAlO_3$ (LAO)(001) and $SrLaAlO_4$ (SLAO)(001) substrates, which exhibit nominal lattice mismatches of approximately −1.1% and −2%, respectively, as depicted schematically in Fig. 1(a). The negative values indicate that the films experience compressive strain during growth. The film growth was carefully monitored via *in situ* reflection high-energy electron diffraction (RHEED). Figure 1(b) illustrates RHEED images of the SLAO(001) substrate (left) and the STO/$LNO_{327}$ film on SLAO (right).

A single-unit-cell STO capping layer was deposited to protect the underlying $LNO_{327}$ from degradation during subsequent experimental procedures. Well-defined Kikuchi lines observed on the bare substrate confirm its single-crystalline nature and surface smoothness. Furthermore, the streaklike RHEED pattern recorded for the film in both zeroth- and first-order diffraction [Fig. 1(b), right] attest to the epitaxial growth of the film. Figures 1(c) and 1(d) display the x-ray diffraction (XRD) $\theta - 2\theta$ symmetric scans for $LNO_{327}$ films on SLAO and LAO substrates, respectively. Distinct $(00l)$ diffraction peaks associated with the bilayer $LNO_{327}$ (n = 2 in $Ln_{n+1}Ni_nO_{3n+1}$) Ruddlesden-Popper structure are evident, notably the (008) and (0012) reflection, whose intensity has previously been linked to the superconductivity [7]. The extracted out-of-plane $c$-axis lattice constant for the $LNO_{327}$ film was determined to be 20.35 Å for the SLAO substrate

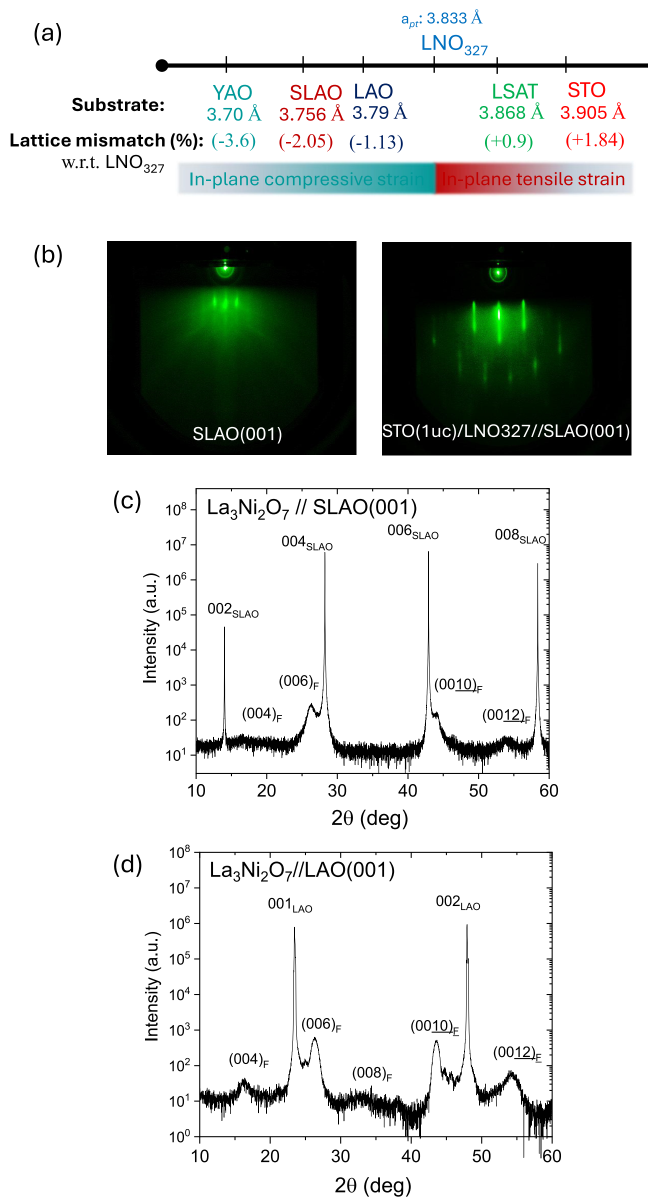


FIG. 1. (a) Schematic representation of lattice mismatch between $LNO_{327}$ and various oxide substrates. (b) Reflection high-energy electron diffraction (RHEED) patterns for the bare SLAO(001) substrate (left panel) and that of the film hetrostructure (right panel). (c), (d) X-ray diffraction (XRD) $\theta - 2\theta$ scans for $LNO_{327}$ films on SLAO(001) and LAO(001) substrates, respectively. The $(00l)_F$ diffraction peaks belong to the $LNO_{327}$ thin film.

and 20.25 Å for the LAO substrate. These values are consistent with prior studies of superconducting $LNO_{327}$ films, indicating that the films are fully strained with the substrates, with more compressively mismatched SLAO substrate producing longer out-of-plane lattice constant. The synthesis of $LNO_{327}$ films is highly sensitive to the kinetic parameters and ambient oxygen partial pressure during deposition, necessitating operation within a narrowly defined growth window to achieve the desired phase formation.

Figure 2 presents the transport measurements of $LNO_{327}$ films on LAO(001) [Figs. 2(a) and 2(b)] and SLAO(001)

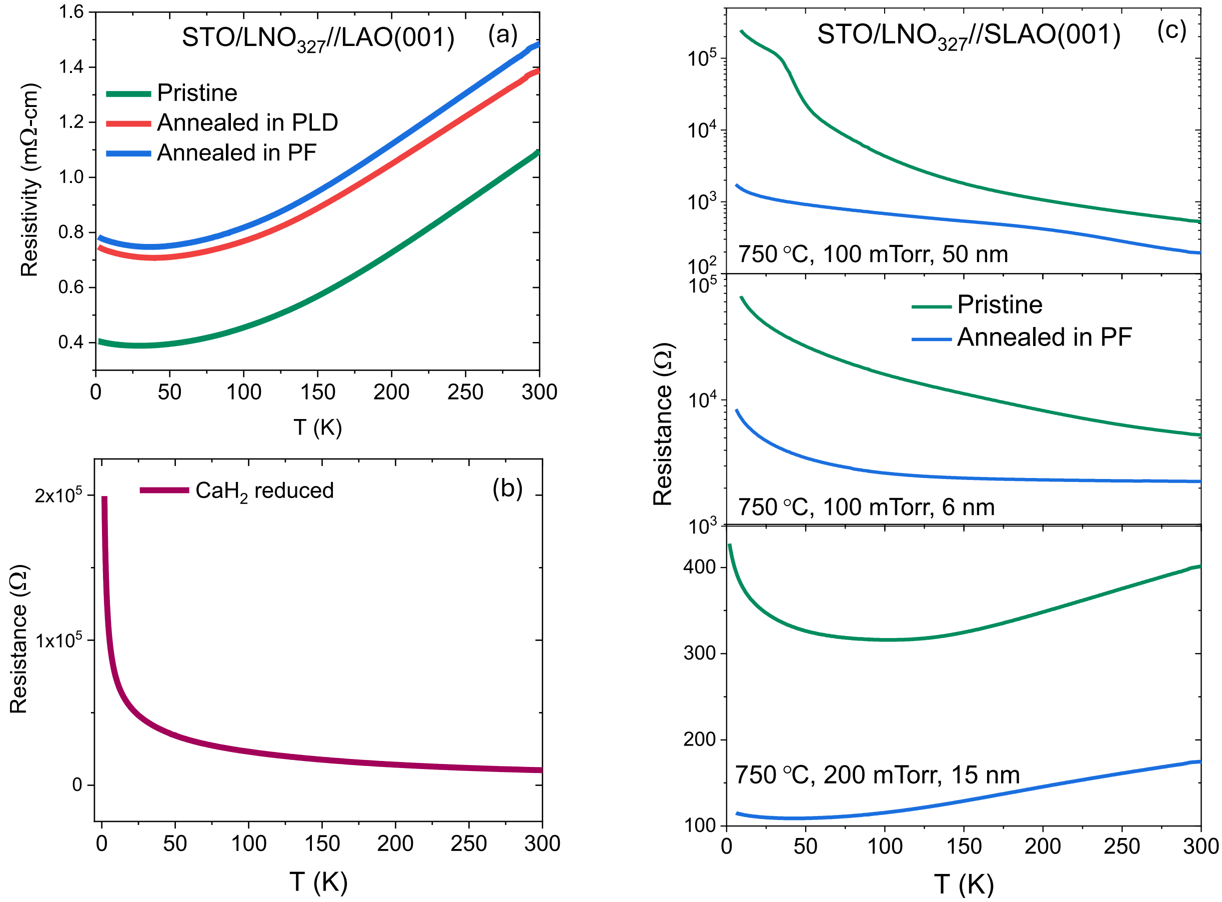


FIG. 2. (a) Resistivity vs temperature plots for the as-grown $LNO_{327}$ film on LAO(001) and the corresponding scans for the annealed films in *in situ* PLD (at 300 torr, 650°C) and in high-pressure furnace (PF) (at 15 bar, 650°C) for 18 h. Temperature dependence of resistance for (b) topotactically reduced $LNO_{327}$ thin film on LAO substrate, (c) pristine and annealed $LNO_{327}$ films on the SLAO(001) substrate. Annealing of films on SLAO(001) substrate was performed in pressure furnace at 15 bar, 650°C for 18 h.

[Fig. 2(c)] substrates. The film grown on an LAO substrate demonstrates typical Fermi-liquid metallic behavior, consistent with previous studies [8,11]. Since nickelate thin films are often affected by oxygen deficiencies [7,8,12,13], additional annealing was conducted both *in situ* in the PLD chamber and in a furnace under high oxygen pressure to replenish possible oxygen deficiency. Following these treatments, the resistivity of the $LNO_{327}$ film on LAO substrate doubled; however, its resistance-temperature characteristics remained unaltered. The observed increase in resistance may also result from changes in contact resistance.

To further investigate the effects of reduction, the sample was topotactically reduced by sealing it in a Pyrex glass tube with approximately 0.1 g of $CaH_2$ powder and heating at 300°C for two hours. This procedure parallels the reduction used to obtain the infinite-layer nickelate with superconducting properties ($T_c \sim$ 15–20 K) from the standard perovskite 113 phase [1,14]. After the reduction, the film turns insulating as anticipated for oxygen-deficient $LNO_{327}$ films [9]. Figure 2(c) displays four-point-probe resistance-temperature plots for pristine and annealed $LNO_{327}$ films on SLAO(001) substrates, grown under varying oxygen pressures and film thicknesses. The pristine films grown at lower oxygen pressure show insulating behavior [Fig. 2(c), top and middle panels], whereas the film grown at higher pressure exhibits a metal-to-insulator transition [Fig. 2(c), bottom panel]. This finding supports previous reports [7,8] and confirms that a precise growth partial pressure—specifically around 100 mtorr—is required to produce pure bilayer $LNO_{327}$ films [see Fig. 1(c) and Fig. 1(d)]. If the oxygen partial pressure is higher, the competing $LaNiO_3$ phase forms instead, which exhibits metallic properties in normal state transport. Following the annealing process, films grown at lower pressures continue to exhibit insulating behavior [Fig. 2(c), top and middle panels], whereas the film synthesized at higher pressure demonstrates increased metallicity [Fig. 2(c), bottom panel]. Notably, despite annealing under elevated oxygen pressures, the films largely retain their insulating nature—particularly those grown at lower partial pressures where improved conductivity would be anticipated considering oxygen vacancies have been filled. This result contrasts with observations in ozone-annealed $LNO_{327}$ thin films on SLAO(001) substrates, which transition to a superconducting state post-ozone annealing process [5–8]. The persistence of insulating behavior may stem from incomplete oxygenation of the films, potentially indicating a need for extended annealing durations under high pressure. These findings underscore the importance of carefully regulated ozone exposure for $LNO_{327}$ thin films, a

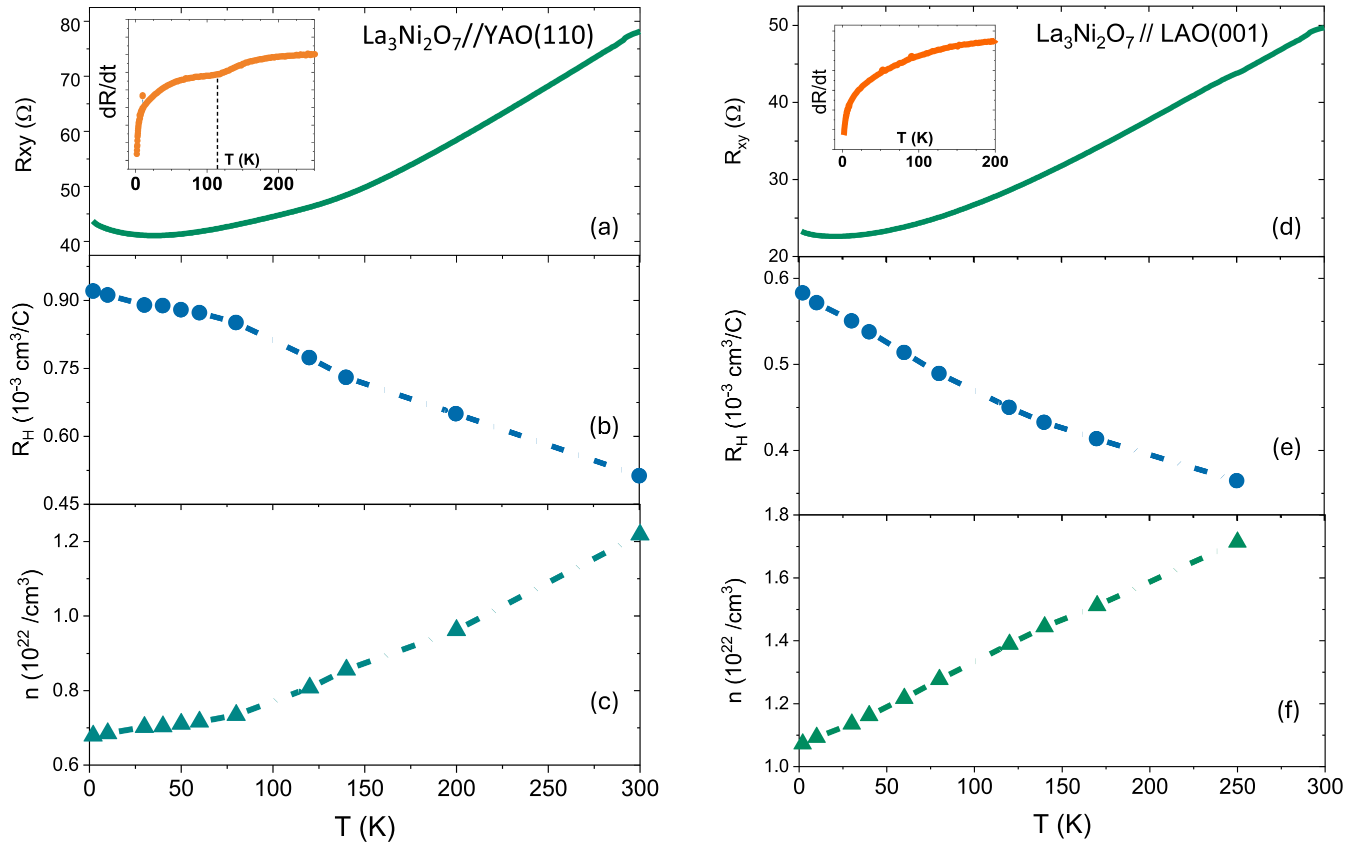


FIG. 3. Hall effect measurements for $LNO_{327}$ films on the YAO(110) and LAO(001) substrates; (a) Sheet resistance, (b) Hall coefficient ($R_H$), (c) carrier concentration ($n$) plotted as a function of temperature for the $LNO_{327}$ film on YAO(110) substrate. (d) Sheet resistance, (e) Hall coefficient, (f) carrier concentration plotted with temperature for $LNO_{327}$ film on the LAO(001) substrate. The dashed line shows transition around 117 K, and is only guide to the eyes.

process after which the films start to display the superconducting properties.

Next, we present Hall effect measurements conducted on the $LNO_{327}$ thin films deposited on $YAlO_3$ (YAO)(110) and LAO(001) substrates (Fig. 3), using a Van der Pauw wiring configuration and magnetic field applied perpendicular to the sample surface. Figure 3(a) displays the sheet resistance $R_{xy}$ as a function of temperature for the film on YAO(110), accompanied by its derivative to emphasize the transition [inset, Fig. 3(a)]. Both the derivative and the raw resistance-temperature data exhibit a pronounced kink near 120 K, suggesting a transition at this temperature. To corroborate this observation, we performed Hall measurements by performing magnetic-field-dependent Hall resistance of $LNO_{327}$ films measured between 2K and 300 K (not shown here) and extracted the Hall coefficient [$R_H$, Fig. 3(b)] and carrier concentration [$n$, Fig. 3(c)]. As shown in Fig. 3(b), the calculated Hall coefficient $R_H$ is positive at measured temperatures and decreases with increasing temperature. Such behavior may indicate multiband electronic structure of the $LNO_{327}$ films, where electronic structure near the Fermi surface is dominated by Ni 3$d$ orbitals ($3d_{z^2}$ and $3d_{x^2-y^2}$) and is consistent with previous results [7,8,15]. Notably, both $n$ and $R_H$ deviate from linearity in temperature around the same temperature where a transition is observed in the resistance-temperature measurements. For comparison, analogous measurements were carried out on a film grown on the LAO substrate, which has a lower lattice mismatch; these results demonstrate a typical metallic resistance-temperature curve [Fig. 3(d)] with no indication of a corresponding transition. Furthermore, Hall effect data for this sample reveal an almost linear dependence of $n$ and $R_H$ on temperature. Similar transitions have been reported for nickelate thin films and single crystals, and were attributed to the spin density wave (SDW) ordering mechanisms [11,16–19]. Recent studies have demonstrated that $LNO_{327}$ single crystals at ambient pressure exhibit the SDW order below 150 K, as evidenced by the resonant inelastic x-ray scattering and nuclear magnetic resonance measurements [16,18]. This observation could explain the analogous ordering observed in $LNO_{327}$ films grown on YAO(110) substrates [Fig. 3(a)]. Owing to a substantial lattice mismatch of −3.6%, the film on the YAO substrate should be largely relaxed, thereby closely replicating the behavior of its bulk counterpart. In contrast, the film grown on the LAO substrate should be fully strained due to a smaller lattice mismatch, where the SDW state is either weakened or not observable in the current transport setup. However, previous work on $La_3Ni_2O_7$ thin film on LAO revealed an SDW ordered phase probed by using resonant soft x-ray scattering [11]. This behavior resembles that seen in the iron-based [20,21] and heavy-fermion superconductors [22,23] where a distinct SDW anomaly is present in the bulk but becomes broadened as a result of epitaxial strain

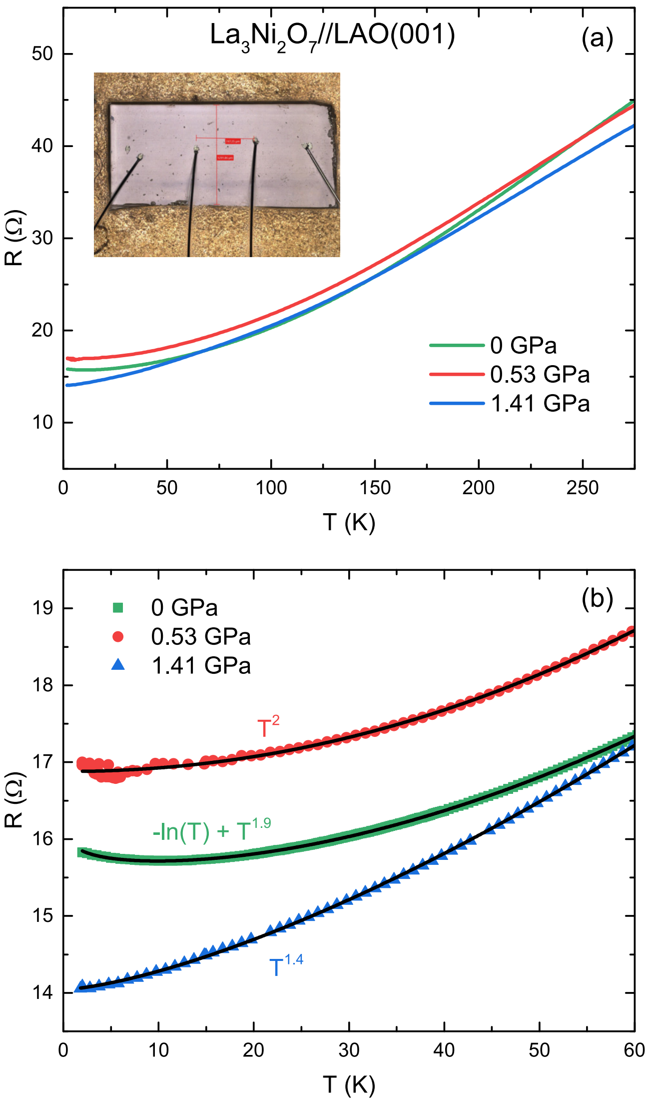


FIG. 4. (a) Resistance vs temperature scans for the $LNO_{327}$ film on LAO(001) substrate under pressure. (b) Power-law fits to the data at low temperature. The symbols represent data points and the black lines represent the fits. The $T$ dependence changes from $T^2$ at 0.53 GPa to $T^{1.4}$ at 1.41 GPa.

in thin films. Therefore, alternative techniques such as magnetic torque or nuclear magnetic resonance (NMR) may be necessary to detect the SDW transition. Additional experiments are warranted to elucidate the nature of the ordering at this transition.

We now address the pressure dependence of transport measurements in $LNO_{327}$ film grown on LAO(001) substrate. Figure 4(a) presents the temperature-dependent resistance *R(T)* at three pressures: ambient, 0.53 GPa, and 1.41 GPa, measured using a piston-cylinder cell (PCC) with Daphne 7575 oil as the pressure-transmitting medium. The pressure was determined *in situ* with a Pb manometer. The $LNO_{327}$ film exhibits metallic behavior across all pressures examined. The entire *R(T)* curve increases slightly as pressure rises incrementally from ambient pressure to 0.53 GPa, especially below 200 K, which may be attributed to the distortion of the $NiO_6$ octahedra, consistent with previous findings and first-principles investigations [2,24], where 1 GPa pressure changes the ground state from metallic to weakly insulating in the $LNO_{327}$ single crystals. At ambient pressure, a slight upturn in resistance at low temperature emerges at around 10 K, consistent with prior studies [8,25], and is potentially attributable to the Kondo-like scattering mechanisms. Notably, this upturn is suppressed under elevated pressures.

To quantify the curvature changes, power-law fitting was performed on the low-temperature data, as shown in Fig. 4(b). At ambient pressure, the data align best with a Kondo model described by $R \propto -ln(T) + T^{\gamma}$. Under increased pressure, the optimal fit transitions to a simple power law: $R(T) = R_0 + AT^{\alpha}$. Up to 0.53 GPa, the measured power law is consistent with Fermi-liquid behavior, characterized by a $T^2$ dependence of resistance due to quasiparticle-quasiparticle scattering. However, upon further pressure increase this power law evolves to a non-Fermi-liquid behavior, with $\alpha = 1.4$ over an expansive temperature range spanning from 1.8 K to 60 K. A detailed comparison of various fitting models for transport data across different pressures, along with uncertainty estimates for $\alpha$, is provided in the Supplemental Material [26].

Comparable non-Fermi-liquid transport phenomena have been observed in bulk bilayer nickelates at much higher pressures [4,27] along with a theoretical investigation [28], as well as in infinite-layer nickelates [29]. However, the marked decrease in exponent from $\alpha \simeq 2$ (Fermi-liquid) to $\alpha = 1.4$ with very small relative pressure increase is unexpected, given the very large range of pressures previously required to see substantial changes in this system. The hydrostatic pressures applied to our thin films amount to only 6–8% of those utilized with diamond anvil cells on $LNO_{327}$ single crystals to achieve similar effects [2,4,27]. This is very surprising to see such a drastic change in the electronic correlations over a small pressure range, and has not been reported thus far in the $LNO_{327}$ thin films to the best of our knowledge. Several factors may contribute to the observation of such non-Fermi-liquid (NFL) behavior. One possibility is the existence of structural defects or phase transitions occurring under hydrostatic pressure, which could induce spatial fluctuations in electron interactions. These fluctuations may suppress the long-lived quasiparticles and consequently lead to NFL behavior [30]. Secondly, given the *in situ* strain tuning of thin film by the underlying mismatched substrate, in addition to the application of the hydrostatic pressure, the $La_3Ni_2O_7$ thin film might lie proximate to the quantum critical point (QCP) of the SDW ordered phase [11]. The behavior observed here is in fact very comparable to that observed in infinite-layer nickelates, Fe-based, and cuprate superconductors [31–35]. Here, the level of epitaxial strain could tune $LNO_{327}$ thin film very close to the SDW phase at ambient pressure, requiring only a few GPa of applied pressure to tune closest to the QCP.

For spin fluctuation scattering, the theoretical value of the temperature exponent depends on the nature and dimensionality of the magnetism of the proximate ordered phase, ranging from superlinear in two-dimensional ferromagnetic ($\alpha = 4/3$) and three-dimensional antiferromagnetic ($\alpha = 3/2$) systems to linear ($\alpha = 1$) in 2D AFM systems [36]. While measurements over a wider pressure range are required to understand the quantitative distance to the critical point itself, the rapid change in power law suggests that $\alpha = 1.4$ is rapidly approaching the limiting power close to the QCP itself. Because a linear exponent has been repeatedly observed in other nickelate systems [29,31,37], it is likely that this system is expected to approach similar behavior at slightly higher pressures as well, consistent with a scenario where quantum criticality is tuning the unconventional normal state behavior and possibly instigating the superconductivity itself. Further fine tuning of strain, oxygen annealing and pressures will indicate if superconductivity itself can be observed to emerge along with such tuning.

## IV. CONCLUSIONS

In summary, we have achieved the epitaxial growth of $La_3Ni_2O_7$ thin films on various oxide substrates and subsequently annealed them in an oxygen-rich environment, rather than utilizing ozone. Our findings show that simply annealing the films in oxygen, regardless of its richness, is not enough to induce superconductivity; ozone appears to be necessary for promptly filling oxygen vacancies in the $La_3Ni_2O_7$ films. Ozone, as a highly reactive form of oxygen, appears to replenish lost oxygen during film growth much more efficiently than the molecular oxygen, which may require several days to achieve comparable compensation. The Hall-effect measurements were performed for $La_3Ni_2O_7$ films on $LaAlO_3$ (001) and $YAlO_3$ (110). A transition potentially associated with a spin density wave has been identified in the Hall measurements of $La_3Ni_2O_7$ film on a YAO(110) substrate. Moreover, pressure-dependent transport measurements were performed on $La_3Ni_2O_7$ film on the $LaAlO_3$ (001). Our results demonstrate that at ambient pressure, the film exhibits a slight upturn in low-temperature resistance, which fits well to a logarithmic Kondo model. Under elevated pressure, this upturn vanishes, and the temperature-dependent resistance can be best fitted to a power law of the form $R(T) = R_0 + AT^{\alpha}$ with $\alpha = 2$ (Fermi-liquid) at 0.52 GPa, and $\alpha \sim 1.4$ (non-Fermi-liquid) at 1.41 GPa. These observations suggest the role of epitaxial strain accompanied by the hydrostatic pressure in tuning the electronic correlations in $La_3Ni_2O_7$ thin films, resulting in the change in the low-temperature transport behavior at elevated hydrostatic pressures, which is merely 6–8 % of the pressure applied with diamond anvil cells in $La_3Ni_2O_7$ single crystals to observe similar phenomena.

## ACKNOWLEDGMENTS

The authors acknowledge R. L. Greene, T. Sarkar, and S. R. Saha for discussions and assistance. This work was supported by the Gordon and Betty Moore Foundation's EPiQS Initiative Grant No. GBMF9071, the U.S. National Science Foundation Grant No. DMR2303090, the Air Force Office of Scientific Research Grant No. FA9950-22-1-0023, the National Science Foundation DMREF program Grant No. DMR2523217, the Breakthrough Energy Fellows program, the NIST Center for Neutron Research, and the Maryland Quantum Materials Center.

## DATA AVAILABILITY

The data that support the findings of this article are not publicly available upon publication because it is not technically feasible and/or the cost of preparing, depositing, and hosting the data would be prohibitive within the terms of this research project. The data are available from the authors upon reasonable request.

[1] D. Li, K. Lee, B. Y. Wang, M. Osada, S. Crossley, H. R. Lee, Y. Cui, Y. Hikita, and H. Y. Hwang, Superconductivity in an infinite-layer nickelate, Nature (London) **572**, 624 (2019).

[2] H. Sun, M. Huo, X. Hu, J. Li, Z. Liu, Y. Han, L. Tang, Z. Mao, P. Yang, B. Wang, J. Cheng, D. X. Yao, G. M. Zhang, and M. Wang, Signatures of superconductivity near 80 K in a nickelate under high pressure, Nature (London) **621**, 493 (2023).

[3] X. Chen, J. Zhang, A. S. Thind, S. Sharma, H. LaBollita, G. Peterson, H. Zheng, D. P. Phelan, A. S. Botana, R. F. Klie, and J. F. Mitchell, Polymorphism in the Ruddlesden–Popper nickelate $La_3Ni_2O_7$: Discovery of a hidden phase with distinctive layer stacking, J. Am. Chem. Soc. **146**, 3640 (2024).

[4] N. Wang, G. Wang, X. Shen, J. Hou, J. Luo, X. Ma, H. Yang, L. Shi, J. Dou, J. Feng, J. Yang, Y. Shi, Z. Ren, H. Ma, P. Yang, Z. Liu, Y. Liu, H. Zhang, X. Dong, Y. Wang, *et al.*, Bulk high-temperature superconductivity in pressurized tetragonal $La_2PrNi_2O_7$, Nature (London) **634**, 579 (2024).

[5] B. Hao, M. Wang, W. Sun, Y. Yang, Z. Mao, S. Yan, H. Sun, H. Zhang, L. Han, Z. Gu, J. Zhou, D. Ji, and Y. Nie, Superconductivity in Sr-doped $La_3Ni_2O_7$ thin films, Nat. Mater. **24**, 1756 (2025).

[6] H. Ji, Z. Xie, Y. Chen, G. Zhou, L. Pan, H. Wang, H. Huang, J. Ge, Y. Liu, G. M. Zhang, Z. Wang, Q. K. Xue, Z. Chen, and J. Wang, Time-reversal symmetry breaking superconductivity with electronic glass in nickelate (La, Pr, Sm)$_3Ni_2O_7$ films, arXiv:2508.16412.

[7] Y. Liu, E. K. Ko, Y. Tarn, L. Bhatt, J. Li, V. Thampy, B. H. Goodge, D. A. Muller, S. Raghu, Y. Yu, and H. Y. Hwang, Superconductivity and normal-state transport in compressively strained $La_2PrNi_2O_7$ thin films, Nat. Mater. **24**, 1221 (2025).

[8] E. K. Ko, Y. Yu, Y. Liu, L. Bhatt, J. Li, V. Thampy, C. T. Kuo, B. Y. Wang, Y. Lee, K. Lee, J. S. Lee, B. H. Goodge, D. A. Muller, and H. Y. Hwang, Signatures of ambient pressure superconductivity in thin film $La_3Ni_2O_7$, Nature (London) **638**, 935 (2025).

[9] M. Osada, C. Terakura, A. Kikkawa, M. Nakajima, H. Y. Chen, Y. Nomura, Y. Tokura, and A. Tsukazaki, Strain-tuning for superconductivity in $La_3Ni_2O_7$ thin films, Commun. Phys. **8**, 251 (2025).

[10] A. Biswas, P. B. Rossen, J. Ravichandran, Y. H. Chu, Y. W. Lee, C. H. Yang, R. Ramesh, and Y. H. Jeong, Selective A- or B-site single termination on surfaces of layered oxide $SrLaAlO_4$, Appl. Phys. Lett. **102**, 051603 (2013).

[11] N. K. Gupta, R. Gong, Y. Wu, M. Kang, C. T. Parzyck, B. Z. Gregory, N. Costa, R. Sutarto, S. Sarker, A. Singer, D. G. Schlom, K. M. Shen, and D. G. Hawthorn, Anisotropic spin stripe domains in bilayer $La_3Ni_2O_7$, Nat. Commun. **16**, 6560 (2025).

[12] C. Lu, M. Zhang, Z. Pan, C. Wu, and F. Yang, Impact of pressure and apical oxygen vacancies on superconductivity in $La_3Ni_2O_7$, Commun. Phys. **8**, 354 (2025).

[13] G. Zhou, W. Lv, H. Wang, Z. Nie, Y. Chen, Y. Li, H. Huang, W. Q. Chen, Y. J. Sun, Q. K. Xue, and Z. Chen, Ambient-Pressure Superconductivity Onset above 40 K in (La, Pr)$_3$Ni$_2$O$_7$ films, Nature (London) **640**, 641 (2025).

[14] M. Osada, B. Y. Wang, K. Lee, D. Li, and H. Y. Hwang, Phase diagram of infinite layer praseodymium nickelate $Pr_{1-x}Sr_xNiO_2$ thin films, Phys. Rev. Mater. **4**, 121801(R) (2020).

[15] X. Hu, W. Qiu, C. Q. Chen, Z. Luo, and D. X. Yao, Electronic structures and multi-orbital models of $La_3Ni_2O_7$ thin films at ambient pressure, Commun. Phys. **8**, 506 (2025).

[16] D. Zhao, Y. Zhou, M. Huo, Y. Wang, L. Nie, Y. Yang, J. Ying, M. Wang, T. Wu, and X. Chen, Pressure-enhanced spin-density-wave transition in double-layer nickelate $La_3Ni_2O_{7-\delta}$, Sci. Bull. **70**, 1239 (2025).

[17] R. Khasanov, T. J. Hicken, D. J. Gawryluk, V. Sazgari, I. Plokhikh, L. P. Sorel, M. Bartkowiak, S. Botzel, F. Lechermann, I. M. Eremin, H. Luetkens, and Z. Guguchia, Pressure-enhanced splitting of density wave transitions in $La_3Ni_2O_{7-\delta}$, Nat. Phys. **21**, 430 (2025).

[18] X. Chen, J. Choi, Z. Jiang, J. Mei, K. Jiang, J. Li, S. Agrestini, M. Garcia-Fernandez, H. Sun, X. Huang, D. Shen, M. Wang, J. Hu, Y. Lu, K. J. Zhou, and D. Feng, Electronic and magnetic excitations in $La_3Ni_2O_7$, Nat. Commun. **15**, 9597 (2024).

[19] K. Chen, X. Liu, J. Jiao, M. Zou, C. Jiang, X. Li, Y. Luo, Q. Wu, N. Zhang, Y. Guo, and L. Shu, Evidence of spin density waves in $La_3Ni_2O_{7-\delta}$, Phys. Rev. Lett. **132**, 256503 (2024).

[20] M. Rotter, M. Tegel, I. Schellenberg, W. Hermes, R. Pottgen, and D. Johrendt, Spin density wave anomaly at 140 K in the ternary iron arsenide $BaFe_2As_2$, Phys. Rev. B **78**, 020503(R) (2008).

[21] J. Engelmann, V. Grinenko, P. Chekhonin, W. Skrotzki, D. V. Efremov, S. Oswald, K. Iida, R. Huhne, J. Hanisch, M. Hoffmann, F. Kurth, L. Schultz, and B. Holzapfel, Strain induced superconductivity in the parent compound $BaFe_2As_2$, Nat. Commun. **4**, 2877 (2013).

[22] A. D. Christianson, A. H. Lacerda, M. F. Hundley, P. G. Pagliuso, and J. L. Sarrao, Magnetotransport of $CeRhIn_5$, Phys. Rev. B **66**, 054410 (2002).

[23] J. Kim, H. Lee, S. Lee, S. Park, T. Park, Y. Cho, H. Lee, W. N. Kang, and W. S. Choi, Synthesis of heavy fermion $CeCoIn_5$ thin film via pulsed laser deposition, Curr. Appl. Phys. **19**, 1338 (2019).

[24] Y. Mochizuki, H. Akamatsu, Y. Kumagai, and F. Oba, Strain-engineered Peierls instability in layered perovskite $La_3Ni_2O_7$ from first principles, Phys. Rev. Mater. **2**, 125001 (2018).

[25] T. Cui, S. Choi, T. Lin, C. Liu, G. Wang, N. Wang, S. Chen, H. Hong, D. Rong, Q. Wang, Q. Jin, J. O. Wang, L. Gu, C. Ge, C. Wang, J. G. Cheng, J. Q. Zhang, L. Si, K. Jin, and E. J. Guo, Strain-mediated phase crossover in Ruddlesden–Popper nickelates, Commun. Mater. **5**, 32 (2024).

[26] See Supplemental Material at http://link.aps.org/supplemental/10.1103/zjnc-vv8p for comparison of various fitting models for transport data across different pressures.

[27] Y. Zhang, D. Su, Y. Huang, Z. Shan, H. Sun, M. Huo, K. Ye, J. Zhang, Z. Yang, Y. Xu, Y. Su, R. Li, M. Smidman, M. Wang, L. Jiao, and H. Yuan, High-temperature superconductivity with zero resistance and strange-metal behaviour in $La_3Ni_2O_{7-\delta}$, Nat. Phys. **20**, 1269 (2024).

[28] S. Onari, D. Inoue, R. Tazai, Y. Yamakawa, and H. Kontani, Impact of multiband effects on non-Fermi-liquid transport phenomena in bilayer nickelates, Phys. Rev. B **113**, 245110 (2026).

[29] K. Lee, B. Y. Wang, M. Osada, B. H. Goodge, T. C. Wang, Y. Lee, S. Harvey, W. J. Kim, Y. Yu, C. Murthy, S. Raghu, L. F. Kourkoutis, and H. Y. Hwang, Linear-in-temperature resistivity for optimally superconducting (Nd, Sr)$NiO_2$, Nature (London) **619**, 288 (2023).

[30] E. Miranda, V. Dobrosavljevic, and G. Kotliar, Disorder-driven non-Fermi-liquid behavior in Kondo alloys, Phys. Rev. Lett. **78**, 290 (1997).

[31] D. Li, B. Y. Wang, K. Lee, S. P. Harvey, M. Osada, B. H. Goodge, L. F. Kourkoutis, and H. Y. Hwang, Superconducting dome in $Nd_{1-x}Sr_xNiO_2$ infinite layer films, Phys. Rev. Lett. **125**, 027001 (2020).

[32] N. N. Wang, M. W. Yang, Z. Yang, K. Y. Chen, H. Zhang, Q. H. Zhang, Z. H. Zhu, Y. Uwatoko, L. Gu, X. L. Dong, J. P. Sun, K. J. Jin, and J. G. Cheng, Pressure-induced monotonic enhancement of $T_c$ to over 30 K in superconducting $Pr_{0.82}Sr_{0.18}NiO_2$ thin films, Nat. Commun. **13**, 4367 (2022).

[33] C. M. Duffy, S. J. Tu, Q. H. Chen, J. S. Zhang, A. Cuoghi, R. D. H. Hinlopen, T. Sarkar, R. L. Greene, K. Jin, and N. E. Hussey, Evidence for spin-fluctuation-mediated superconductivity in electron-doped cuprates, arXiv:2502.13612.

[34] H. Kontani, Anomalous transport phenomena in Fermi liquids with strong magnetic fluctuations, Rep. Prog. Phys. **71**, 026501 (2008).

[35] W. K. Huang, S. Hosoi, M. Culo, S. Kasahara, Y. Sato, K. Matsuura, Y. Mizukami, M. Berben, N. E. Hussey, H. Kontani, T. Shibauchi, and Y. Matsuda, Non-Fermi liquid transport in the vicinity of the nematic quantum critical point of superconducting $FeSe_{1-x}S_x$, Phys. Rev. Res. **2**, 033367 (2020).

[36] G. R. Stewart, Non-Fermi-liquid behavior in $d$- and $f$-electron metals, Rev. Mod. Phys. **73**, 797 (2001).

[37] S. Hiragami and S. Onari, Non-Fermi-liquid transport phenomena in infinite-layer nickelates, J. Phys. Soc. Jpn. **94**, 124706 (2025).